

Sustained Efficacy and Arterial Drug Retention by a Fast Drug Eluting Cross-Linked Fatty Acid Coronary Stent Coating

NATALIE ARTZI,^{1,2} ABRAHAM R. TZAFRIRI,^{1,3} KEITH M. FAUCHER,⁴ GEOFFREY MOODIE,⁴ THERESA ALBERGO,⁴ SUZANNE CONROY,⁴ SCOTT CORBEIL,⁴ PAUL MARTAKOS,⁴ RENU VIRMANI,⁵ and ELAZER R. EDELMAN^{1,6}

¹Institute for Medical Engineering and Science, Massachusetts Institute of Technology, Cambridge, MA, USA; ²Department of Anesthesiology, Brigham and Women's Hospital, Harvard Medical School, Boston, MA, USA; ³Department of Applied Science, CBSET Inc., Lexington, MA, USA; ⁴MAQUET Vascular Systems (Formerly Atrium Medical Corporation), 40 Continental Blvd., Merrimack, NH 03054, USA; ⁵CV Path Institute, 19 Firstfield Road, Gaithersburg, MD 20878, USA; and

⁶Cardiovascular Division, Brigham and Women's Hospital, Harvard Medical School, Boston, MA, USA

(Received 16 May 2015; accepted 18 August 2015)

Associate Editor Sean McGinty oversaw the review of this article.

Abstract—The long held assumption that sustained drug elution from stent coatings over weeks to months is imperative for clinical efficacy has limited the choice for stent coating materials. We developed and evaluated an omega-3 fatty acid (O3FA) based stent coating that is 85% absorbed and elutes 97% of its Sirolimus analog (Corolimus) load within 8d of implantation. O3FA coated stents sustained drug levels in porcine coronary arteries similarly to those achieved by slow-eluting durable coated Cypher Select Plus Stents and with significantly lower levels of granuloma formation and luminal stenosis. Computational modeling confirmed that diffusion and binding constants of Corolimus and Sirolimus are identical and explained that the sustained retention of Corolimus was facilitated by binding to high affinity intracellular receptors (FKBP12). First in man outcomes were positive—unlike Cypher stents where late lumen loss drops over 6 month, there was a stable effect without diminution in the presence of O3FA. These results speak to a new paradigm whereby the safety of drug eluting stents can be optimized through the use of resorbable biocompatible coating materials with resorption kinetics that coincide with the dissociation and tissue elimination of receptor-bound drug.

Keywords—Drug eluting stents, Sirolimus analogs, Computational modeling.

Address correspondence to Abraham R. Tzafiriri, Department of Applied Science, CBSET Inc., Lexington, MA, USA. Electronic mails: ramitz@mit.edu and rtzafiriri@cbset.org

Natalie Artzi and Abraham R. Tzafiriri have contributed equally to this work.

INTRODUCTION

The idea to combine the principles of mechanical scaffolding and local pharmacological action emerged early in the stent era and has continued to generate interest and dominate interventional use since. However, evidence from animal models and human necropsy studies suggested that drug eluting stents (DES) can delay arterial healing and serve as loci for late thrombosis⁹ and late restenosis^{7,25} potentially related to the drug, the polymer, or both. Though the two drugs most used in DES, Paclitaxel and Sirolimus, both avidly bind arterial tissue,²² fibrin content, a marker for delayed healing, is significantly higher for Paclitaxel eluting relative to Sirolimus eluting stents (SES).^{6,9,25} This has been attributed to the slow elution of Paclitaxel from these devices^{6,9,25} and its ability to sustainably inhibit cell proliferation and migration even after short exposures.² By contrast, SES have been associated with higher rates of late inflammation, hypersensitivity and granulomas.^{25–27} The peaking and persistence of hypersensitivity reactions after complete release of Sirolimus suggested that they represent an adverse effect to polymeric components of the coating. This interpretation was supported by the wide experience with oral Sirolimus for transplant rejection and reports of adverse inflammatory and giant cell responses to polymeric components of the Cypher coating.²⁶

Experiences with first generation DES inspired the design and adoption of next generation DES. Due to the propensity of Paclitaxel to delay healing, Sirolimus

and its analogs are currently the drugs of choice for coronary stent based elution. Concern for persistent adverse responses to durable polymeric coatings prompted the development of more biocompatible durable polymeric materials or bioerodible coatings that are absorbed over the course of several months¹⁵ and the introduction of lower profile stents with lower surface areas for interactions with tissue and blood. Yet with all the innovations in coating and/or scaffold designs,^{11,15} with few exceptions (e.g., Endeavor Stent¹⁵), approved and emerging SES are designed to slowly elute their drug load with Cypher-like kinetics that aim to ensure sustained drug retention in the artery.

This focus on sustained drug elution has restricted the choice of DES coating materials. In particular, bioerodible polymers that permeabilize quickly during hydrolysis and absorption have been shunned in favor of synthetic polymers that are absorbed over the course of several months,¹⁵ e.g., poly lactic acid, poly glycolic acid, or copolymer or other variations thereof.^{11,15} These materials may produce local irritation due to the release of acidic degradation products¹ and can delay healing and transiently place the artery at increased risk of adverse reaction.¹⁹ The optimum temporal balancing of erosion and drug release still awaits full definition as most erodible scaffolds¹³ and stents with erodible coatings¹⁵ release their entire drug load prior to erosion, maintaining the same diffusive mechanisms to sustain release kinetics but also neces-

sarily prolonging the duration of any adverse polymer effects.

The current study was driven by the hypothesis that coating compositions which degrade rapidly can deliver controlled volumes of drug without loss of biological effect and at reduced periods of tissue vulnerability. To examine this hypothesis, we developed and evaluated a cross-linked omega-3 fatty acid (O3FA) based coating that is 85% absorbed and elutes 97% of its Sirolimus analog (Corolimus) load within 8d of implantation. Evaluation in pig coronary arteries revealed sustained efficacious drug levels that were similar to those achieved by slow eluting durable coated SES and resulted in superior efficacy and more benign tissue response. Computational modeling confirmed that Corolimus distributes in arterial tissue with the same diffusion and binding constants as Sirolimus and explained that its sustained retention after fast elution from the O3FA DES was facilitated by binding to high affinity intracellular receptors (FKBP12). Clinical studies demonstrated improved outcome with minimal and stabilizing late lumen loss.

METHODS

O3FA Drug Eluting Stents (O3FA DES)

Formation of the O3FA DES coating relies on oxidative cross-linking of fish oil (Fig. 1). FTIR analysis (supplemental Fig S1) reveals that cross-links are

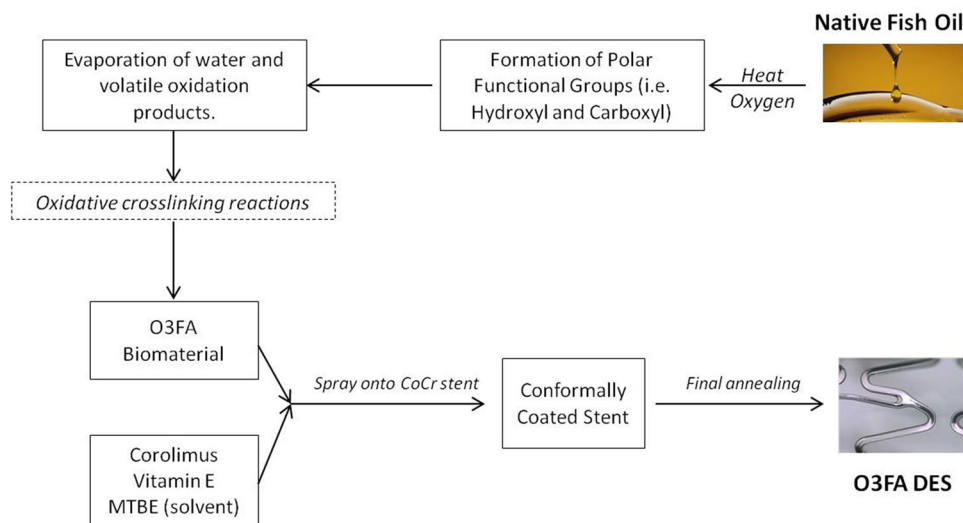


FIGURE 1. Schematics of the process of transforming native fish oil to omega-3 fatty acid based stent coating. Concomitant heating of the native fish oil, infusion and mixing of oxygen into the triglyceride oil leads to oxidative cleavage of the C=C bonds in the oil and predominant formation of hydroxyl and carboxyl functional groups, as supported by FTIR analysis (supplemental Fig S1). Upon further heating during the process, the oil increases in viscosity due to the release of water and volatile oxidation products and the formation of cross-links between the hydroxyl and carboxyl functional groups present in the oil (supplemental Fig S1).

predominantly ester crosslinks and that alkyl chains are in a disordered and non-crystalline state, rendering the coating flexible during stent expansion and deployment.

Fish oil naturally contains a mixture of saturated, monounsaturated, and polyunsaturated oils. Gas Chromatographic fatty acid profile (GC FAP) testing revealed that the polyunsaturated fatty acids of the fish oil form the cross-linked network of the coating (supplemental Fig S2A). The monounsaturated fatty acids are only partially reacted during this process while the saturated fatty acids are nonreactive (supplemental Fig S2A). Comparison of the GC FAP testing to rheometric viscosity measurements revealed that the fatty acid oxidation precedes the rise in viscosity, which correlates with the formation of cross-links between the triglyceride fatty acid chains (supplemental Fig S2A, B). GPC analysis of the starting fish oil and the O3FA biomaterial (supplemental Fig S3) also revealed a significant increase in the average molecular weight from 1000 to 60,000 Daltons, also indicative of crosslinking.

Cinatra™ cobalt chromium stents (Atrium Medical, NH) were spray coated with a mixture of partially cross-linked O3FA, Vitamin E, and Corolimus, a Sirolimus analog. Corolimus, also known as SAR943, is synthesized directly from Sirolimus²⁰ via reduction of the carbonyl of the C32 position of the macrolide ring and was designed to increase the hydrolytic stability of the molecule. The selection of a Corolimus was intended to minimize drug hydrolysis during release and tissue distribution even as the O3FA coating is hydrolyzed.

In Vitro Modeling of O3FA Coating Erosion and Drug Release

In vitro drug elution and coating erosion at 37 °C were correlated using model cobalt chromium shims coated with the same formulation as stents, but with fluorescently labeled O3FA, via integration of 1% NBD-12 Stearate (Invitrogen) into the O3FA material. 20 µL of Atrium's bioabsorbable stent coating based on O3FA, Vitamin E, and containing Corolimus, was pipetted onto the shims and heat cured per the same process as was used on the stents. Triplicate shims were each placed into 5 mL of 0.375% Tween 20 in 0.1 M PBS, pH 6.0 for different time point designated times between 5 min, and 24 h. After extraction was complete, shims were rinsed with DI water and dried in a vacuum chamber, and then weighed and analyzed for remaining fluorescence using IVIS (*In Vivo* Imaging System, Perkin Elmer). The 12-NBD Stearate concentration was then calculated by comparing the observed data to an appropriate calibration curve. The amount of residual coating on the shim was deter-

mined by scanning the samples using IVIS and determining the radiant efficiency. The percentage of residual coating was calculated by normalizing this value to the average efficiency at $t = 0$.

In-vitro Corolimus release was measured by assaying residual drug on the shim via HPLC assay, using a Thermo Surveyor HPLC instrument with UV detection at 278 nm. Samples were extracted in methanol for ~30 min. HPLC analysis was conducted with a C18 column under gradient elution (methanol/0.2% acetic acid) using a C-18 column at 60 °C. The percentage of residual drug was calculated by normalizing this value to the average concentration at $t = 0$.

In-Vivo Coating Erosion and Local Pharmacokinetics of O3FA DES

Both rabbit iliac arteries and porcine coronaries are considered valid models for studying the pharmacokinetics and performance of drug eluting stents.¹⁸ We quantified *in vivo* coating erosion in rabbit iliac arterial implants and local stent pharmacokinetics and biological effects in porcine coronary arteries. All procedures and conditions of testing were performed adherent to the Guide for the Care and Use of Laboratory Animals¹² under an approved Institutional Animal Care and Use Committee protocol, in compliance with the Animal Welfare Act and the Food and Drug Administration Good Laboratory Practice Regulations and their amendments.

O3FA DES Coating Erosion

Radiolabeled O3FA DES (0.257 µCi/stent) were prepared as above, but with integration of an unsaturated triglyceride, ¹⁴C radiolabeled triolein, into the O3FA solution prior to spray coating. At CBSET, Inc. (Lexington, MA) 15 male and female New Zealand White Rabbits underwent a single interventional procedure on Day 0 in which 2 radiolabeled O3FA DES (3.0 × 16 mm) were implanted into each of the common iliac arteries at approximately a 1.1:1 overstretch ratio, under fluoroscopy. Animals were euthanized at designated time points between 5 h, and 90d. The stented iliac arteries were cleaned of surrounding connective tissue, stent and stented tissue were cut longitudinally and the stent carefully separated from the surrounding tissue. Coated stents were exposed to Solvable™ for 4 h at 55 °C. Triplicate ~100 µL weighed aliquots of each extract were mixed with ~5 mL of Hionic Fluor™ (or equivalent) scintillation fluid and counted in a Beckman LS 6500 liquid scintillation counter for 5 min/sample or until a 2-sigma error of <2%. Each vessel segment was weighed, and then solubilized for ≥1 h in a 37–50 °C water bath in

~2 mL of Solvable™ (volume and weight to be recorded). Triplicate ~100 μ L weighed aliquots of each solution were mixed with ~5 mL of Hionic Fluor™ (or equivalent) scintillation fluid and counted in a Beckman LS 6500 liquid scintillation counter for 5 min/sample or until a 2-sigma error of <2%.

Safety Studies

Safety studies were conducted in hybrid Landrace-Yorkshire swine with overlapped exaggerated Corolimus dose O3FA stents (150 μ g/stent), overlapped O3FA stents (9 vessels), and overlapped Cypher Select™ Plus Stents (110 μ g/stent, 8 vessels). Additionally, nominal Corolimus dose O3FA stents (100 μ g/stent), were implanted into porcine coronary vessels ($n = 9$) in a single configuration for 90d. All stents were 13 mm in length and 3.0–3.5 mm in diameter. Implantations were carried out at AccelLab (Boisbriand, Canada) using a 1.1:1 overstretch ratio and a 50% overlap. Animals were sacrificed for analysis at 90d and underwent evaluation by histopathology at CVPPath (Gaithersburg, MD). Additionally, nine vessels implanted with overlapped exaggerated Corolimus dose O3FA were also analyzed at 28d to test for any earlier term toxicities. Evaluation was performed by histopathology and histomorphometry at CVPPath (Gaithersburg, MD).

Pharmacokinetic Analysis

For pharmacokinetic analysis, Cypher Select™ Plus Stents (3.0 \times 13 mm) loaded with 110 μ g Sirolimus and O3FA DES Stents (3.0 \times 13 mm) loaded with 75 μ g Corolimus were implanted in the coronary arteries of Yorkshire swine under angiography (1 stent/artery, 1.1:1 overstretch ratio). At designated time points between 5 h and 141d post-implantation, stented arteries ($n \geq 5$) were harvested and stored frozen on dry ice; subsequently, stents were removed from the stented artery segment and both samples separately prepared for quantification of drug content.

Drug quantification was performed using an Agilent 1100 HPLC coupled to an Applied Biosystems/MDS Sciex 3000 MS/MS at Chemic Laboratories, Inc (Canton, MA). O3FA DES samples were analyzed in multiple reaction mode with transitions of 922.7 \rightarrow 409.4 m/z, 922.7 \rightarrow 441.4 m/z, and 922.7 \rightarrow 209.0 m/z being summed to determine Corolimus concentration. Cypher stents were analyzed in multiple reaction mode with transitions of 936.7 \rightarrow 409.4 m/z and 936.7 \rightarrow 453.3 m/z being summed to determine Sirolimus concentration. Arterial tissue samples were homogenized and extracted with a mixture of hexane and ethyl acetate. The mixtures were centrifuged, the

supernatant decanted, evaporated to dryness, and finally reconstituted in water and acetonitrile. Samples analysis was conducted under isocratic elution (15/70/15% of 10 mM ammonium acetate/isopropyl alcohol/0.1% formic acid in acetonitrile) using an HPLC–MS/MS, C-18 column at 50 °C. Explanted stents were analyzed similarly to tissue, except they were initially extracted in acetonitrile instead of hexane and ethyl acetate.

Histology and Morphometry

At termination of the in-life portion of the study, porcine hearts were perfusion fixed with formalin and sent to CVPPath (Gaithersburg, MD) for histomorphometry and histopathology. Fixed, stented vessels were dissected from the myocardium, sectioned and stained with hematoxylin and eosin and an elastin stain (Movat pentachrome). Light microscopy was used to score the tissue for histopathological variables. Scoring was performed by a board certified pathologist in a blinded fashion. Inflammation and injury were scored on a per strut basis and the average was calculated per plane and per stent. Quantitative morphometric analysis was performed on the histological sections from each stented artery using standard light microscopy and computer-assisted image measurement systems (IP Lab software, Rockville, MD). Lumen area, stent area and areas bounded by the internal and external elastic laminae were all measured directly and used in the calculation of all other morphometric parameters.

Data Analysis and Statistics

Experimental data reported are the mean \pm standard deviation. Dixon's critical Q criterion¹⁷ justified the rejection of only a single outlier data point with 99% confidence (tissue content at 8d with Cypher Select™ Plus). Average *in vivo* cumulative elution data were fit to a biexponential kinetic (Eq. (1)) using GraphPad Prism 3.02. All statistical comparisons were performed with a two-tailed *t* test for independent samples using VassarStats software (VassarCollege). A *p* value of <0.05 was considered to denote statistical significance.

COMPUTATIONAL MODELING OF STENT BASED ARTERIAL DRUG DISTRIBUTION

Drug Elution Kinetics

Cumulative drug release from both DES were fit to bi-exponential kinetics

$$M_{\text{stent}}(t) = M_{\text{stent}}(0) \left[1 - f(1 - e^{-K_f t}) - (1 - f)(1 - e^{-K_s t}) \right] \quad (1)$$

where t denotes time since stent implantation, $M_{\text{stent}}(0)$ is the initial drug load (μg) per stent, f is the fraction of drug in the coating that elutes with a fast rate constant K_f and the remaining fraction elutes with a slower first order rate constant K_s . Results of numerical fits using GraphPad Prism 3.02 are provided in Table 1.

Tissue Content and Receptor Binding

The arterial distribution of Sirolimus and its analog Corolimus is governed by convection, diffusion, non specific, and specific binding. These processes were modeled using the following published equations²⁴

$$\begin{aligned} \partial c / \partial t + \partial b_{\text{ECM}} / \partial t + \partial b_{\text{REC}} / \partial t \\ = D_{\text{wall}} \partial^2 c / \partial r^2 + (D_{\text{wall}} / r) \partial c / \partial r - V_{\text{wall}} \partial c / \partial r, \end{aligned} \quad (2)$$

$$\begin{aligned} \partial b_{\text{ECM}} / \partial t = k_{\text{on}}^{\text{ECM}} c \cdot (b_{\text{ECM}, \text{max}} - b_{\text{ECM}}) \\ - k_{\text{on}}^{\text{ECM}} \cdot K_{\text{d}}^{\text{ECM}} b_{\text{ECM}}, \end{aligned} \quad (3)$$

$$\begin{aligned} \partial b_{\text{REC}} / \partial t = k_{\text{on}}^{\text{REC}} c \cdot (b_{\text{REC}, \text{max}} - b_{\text{REC}}) \\ - k_{\text{on}}^{\text{REC}} \cdot K_{\text{d}}^{\text{REC}} b_{\text{REC}}. \end{aligned} \quad (4)$$

Here r denotes the distance from the intima, c is the molar concentration of free drug per unit tissue volume, b_{ECM} and b_{REC} are the molar concentrations of ECM- and receptor-bound drug, respectively; $b_{\text{ECM}, \text{max}}$ and $b_{\text{REC}, \text{max}}$ denote the local molar concentration of ECM- and receptor drug binding sites, $k_{\text{on}}^{\text{ECM}}$ and $k_{\text{on}}^{\text{REC}}$ are the respective binding on-rate constants, $K_{\text{d}}^{\text{ECM}}$ and $K_{\text{d}}^{\text{REC}}$ are the respective equilibrium dissociation constants, D_{wall} is the transmural diffusivity of the drug and V_{wall} is its transmural convective velocity.

Drug transfer into the artery wall was averaged over the mural interface to obtain a one dimensional prescribed flux condition of the form²⁴

$$\begin{aligned} -D_{\text{wall}} \partial c / \partial r + V_{\text{wall}} c = -f_{\text{wall}} \cdot (dM_{\text{stent}} / dt) \\ / (S_{\text{lumen}} \cdot A_{\text{drug}}), \quad r = r_{\text{min}}. \end{aligned} \quad (5)$$

Here S_{lumen} is the surface area of the blood/wall interface, f_{wall} is the fraction of eluted drug that is transferred to the wall, A_{drug} is the drug's molecular weight and r_{min} is the radius of the expanded stent. The

TABLE 1. Rate constants of bi-exponential drug release (Eq. (1)).

Stent	$M_{\text{stent}}(0)$ (μg)	f	K_f (d^{-1})	K_s (d^{-1})	R^2
Cypher Select™ Plus	110	0.25	7.45	0.052	0.998
O3FA DES	75	0.95	5.26	0.076	1.000

periadventitial surface is assumed to act as a perfect sink for free drug

$$c = 0, \quad r = r_{\text{min}} + W \quad (6)$$

where W denotes the thickness of the arterial wall.

Numerical Methods

Equations (1)–(6) were solved numerically using the commercial finite element package COMSOL 3.5a (COMSOL, Burlington MA) for the parameter values listed in Table 2. The cylindrically symmetric one dimensional computational domain was meshed using 1920 Lagrange cubic elements. The resulting system of algebraic equations was solved with a direct linear solver and integrated using a fifth order backward differencing scheme with variable time stepping and tight tolerances (relative tolerance of 10^{-10} and absolute tolerance of 10^{-12}). Tissue content was evaluated using COMSOL's subdomain integration post processing tool.

RESULTS

In Vitro Drug Release Tracks with Coating Erosion

The degradation kinetics and drug release profile of Corolimus-containing O3FA were examined *in vitro* to understand governing processes in release. *In vitro* release of drug and of the fluorescent coating both

TABLE 2. Arterial-wall transport and equilibrium binding parameters of sirolimus.²⁴

Parameter	Meaning	Estimate
V_{wall}	Transmural velocity	5.8×10^{-6} cm/s
D_{wall}	Transmural diffusivity	2.0×10^{-6} cm ² /s
$b_{\text{ECM}, \text{max}}$ + $b_{\text{REC}, \text{max}}$	Total binding site density	366 μM
$b_{\text{REC}, \text{max}}$	Receptor density	3.3 ± 0.3 μM
$K_{\text{d}}^{\text{ECM}}$	ECM dissociation constant	2.6 μM
$K_{\text{d}}^{\text{REC}}$	Receptor dissociation constant	0.2 nM
$k_{\text{on}}^{\text{ECM}}$	ECM binding on-rate	0.002 $\mu\text{M}^{-1} \text{s}^{-1}$
$k_{\text{on}}^{\text{REC}}$	Receptor binding on-rate	0.8 $\mu\text{M}^{-1} \text{s}^{-1}$
W	Arterial wall thickness	450 μm
r_{min}	Lumen radius	1.5 mm
S_{lumen}	Area of stented lumen	1.22 cm ^{2a}
f_{wall}	Drug transfer efficiency	0.009–0.012 ^b
	Cypher Select™ Plus	0.009
	O3FA DES	0.012
A_{drug}	Sirolimus molecular weight	914.2 g/mol ^c
	Corolimus molecular weight	900.2 ^c

^a Based on stent dimensions, 3.0×13.0 mm.

^b f_{wall} was estimated as the ratio of the weights of tissue associated drug and stent eluted drug at 1 day.²⁴

^c See Strom *et al.*²⁰

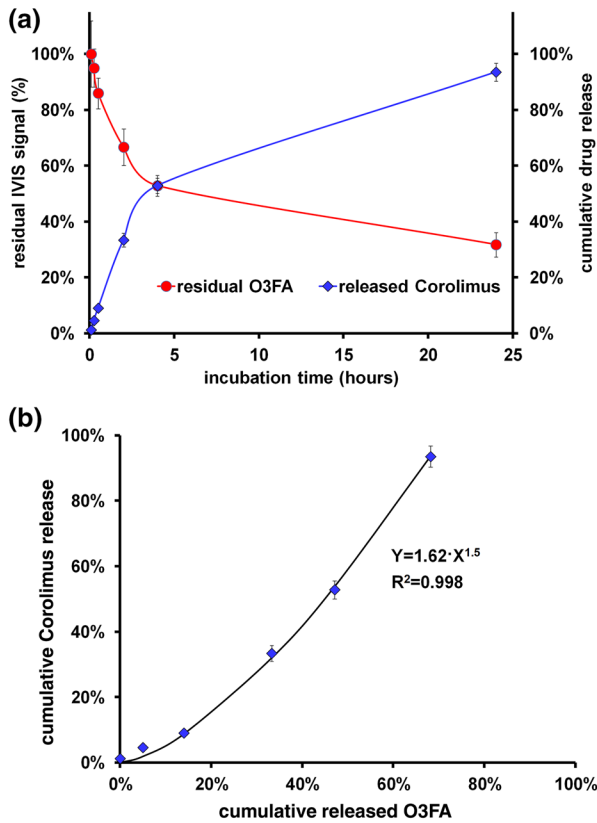


FIGURE 2. Assessing the mechanisms of *in vitro* drug elution from O3FA coatings. (a) Release kinetics of Corolimus (diamonds) and fluorescent coating (circles) from coated shims. (b) Cumulative drug release vs. O3FA degradation.

displayed bi-phasic kinetics that decelerated after 4 h of shim incubation (Fig. 2a). Interestingly, drug release tracked with release of O3FA erosion products once degradation commenced (Fig. 2b) facilitated by the increased permeability levels within the coating following bulk erosion. Drug release from coated shims tracked the *in vitro* release of O3FA DES (supplemental Fig S4), confirming the relevance of the IVIS model.

In Vivo Erosion Kinetics of O3FA DES

In vivo coating erosion of radiolabeled O3FA DES implanted in rabbit iliac arteries exhibited a burst phase followed by a slower kinetic phase (Fig. 3). Coating eroded extremely fast up to 1 h (28.0%/h), more slowly from 1 h up to 8d (7.1%/d) and at a constant rate of 0.1%/d ($R^2 = 0.99$) between 8 and 90d. By 90d, less than 6% of the coating remained on the stent or in the vessel. Notably, tissue exposure to the coating was low throughout the erosion process as <2.4% of the radioactively labeled coating was quantified in the tissue at any time.

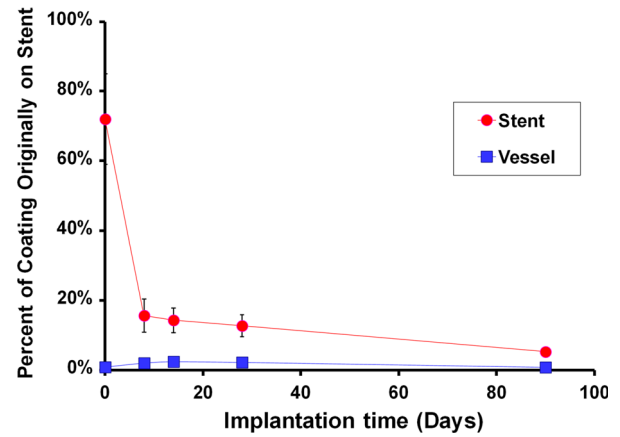


FIGURE 3. *In vivo* absorption of O3FA coating. Stent residual (circles) and tissue absorbed (squares) Radiolabeled O3FA over the course of implantation in rabbit arteries.

In Vivo Pharmacokinetics

Corolimus release from O3FA DES was bi-exponential (Table 1) with more than 60% of the initial load released by 5 h and more than 97.0% by 8d (Fig. 4a). Sirolimus release from Cypher SelectTM Plus SES was also bi-exponential (Table 1) but slower, with only 20% of the initial load released by 5 h and 80.6% by 28d (Fig. 4a). The differential elution kinetics of these DES reflect marked differences in the fractions of their fast eluting drug pools (95 vs. 25%), as both devices displayed comparable fast and slow rate constants of elution (Table 1). Differences in elution kinetics resulted in markedly different early arterial concentrations, but similar sustained levels (Fig. 4b). At 5 h O3FA DES eluted 40% more drug than Cypher SelectTM Plus SES, however, the reverse was true between 8 and 56d, qualitatively tracking the relative rates of drug release. Despite the difference in scaffold design and elution kinetics, only approximately 1% of eluted drug was transferred by O3FA DES and the SES (1.2 vs. 0.9%).

Computational modeling predicted the stent based arterial distribution of Sirolimus and Corolimus using the same set of diffusion and binding constants, but disparate elution kinetics and specific drug transfer efficiencies (Tables 1, 2). Simulations explained that early tissue content is determined by drug diffusion and non specific drug binding interactions, whereas late retention of Sirolimus analogs is critically dependent on the affinity binding to intracellular FKBP12 (Fig. 4b).

Biocompatibility Throughout the Period of O3FA Material Absorption

Safety of the nominal dose O3FA DES in single configuration (Fig. 5a) and exaggerated dose O3FA DES in overlap configuration (Fig. 5b) was compared

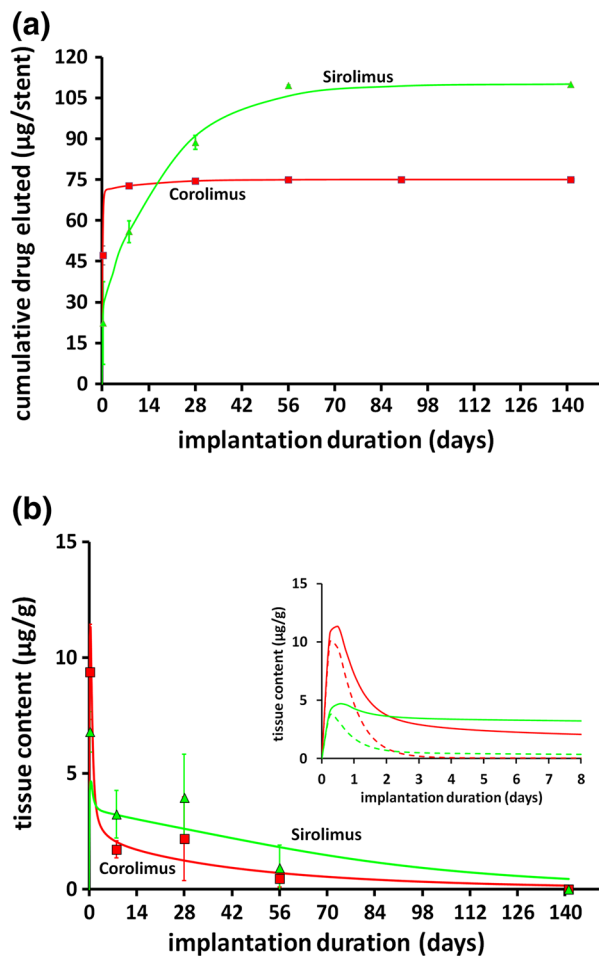


FIGURE 4. Local pharmacokinetics of Cypher Select™ Plus SES (green) and O3FA DES (red). (a) *In vivo* drug release (symbols) follows bi-exponential kinetics (lines, Table 1). (b) *In vivo* tissue content (symbols) is well interpolated by model predictions that account for high affinity drug binding to FKBP12 (lines). Insets highlight early tissue content and also depict simulation results that do not account for high affinity drug binding to FKBP12 (dashes).

to that of Cypher Select™ Plus SES in an overlap configuration at 90d (Fig. 5c).

The porcine coronary artery implant model used involves minimal overstretch that typically shows little neointimal hyperplasia except in the presence of additional stimuli such as pro-inflammatory stent coatings and stent overlap.²⁷ It is therefore notable that implantation of exaggerated dose O3FA DES in the overlap configuration was characterized by benign tissue responses at 28d (Supplemental Fig S5) and by the same low levels of stenosis (Fig. 6a), inflammation (Fig. 6b) and injury (Fig. 6c) as in the single stent configuration and nominal dose, and was superior to overlapped Cypher Select™ Plus SES ($p < 0.01$) at 90d. The high injury and inflammatory scores of overlapped Cypher Select™ Plus SES were associated

with high incidence of granulomas compared to single ($p < 0.01$) and overlapped ($p < 0.01$) O3FA DES, even though the latter eluted 36% more drug than the slow eluting durable coated SES (150 vs. 110 µg/stent). Remarkably, overlapped implantation of exaggerated dose of O3FA was associated with similarly benign tissue response at 28d and absence of any granuloma (Supplemental Fig S5). Given the similarities between Sirolimus and Corolimus, such benign tissue effects are ascribed to the lower inflammatory insult posed by low profile stents that employ biocompatible coatings that absorb over the course of drug elimination from the tissue.

DISCUSSION

The realization that the very coatings that were designed to sustain drug release and optimize efficacy of DES may act as a source of late toxicity fueled the development of designer drug analogs for use in DES coatings, the introduction of biodurable and bioerodible materials for improved biocompatibility relative to first generation coatings, and the adoption of stronger metals that allow for thinner struts and require less coating material. Yet despite the seeming diversity in emerging DES designs, most—including fourth generation stents with bioerodible coatings (e.g., SYNERGY²⁸)—are designed to follow the Cypher SES paradigm of sustained drug elution and tissue retention. The current study illustrates that retention of Sirolimus analogs can be achieved even with fast drug elution kinetics following rapid coating erosion, with computational modeling identifying binding to tissue receptors as the mechanism of prolonged retention. The composition of SES coatings can then be designed for optimal biocompatibility and bioabsorption rather than predominantly for prolonged control of drug elution kinetics. This paradigm shift creates an opportunity for the use of a range of biocompatible materials that may have not otherwise been considered.

Naturally derived biomaterials can offer several advantages over synthetically derived materials, including improvements in the biocompatibility of the material and its degradation products. While naturally derived materials such as cellulose and protein-based materials are commonly used in implantable medical devices, materials created from oils and lipids represent an area of further research and opportunity. The ability to tune the oil fatty acid composition gives rise to biomaterials with a range of physical and chemical properties. In the current study we developed and evaluated a stent coating based on O3FA materials that can readily incorporate hydrophobic compounds

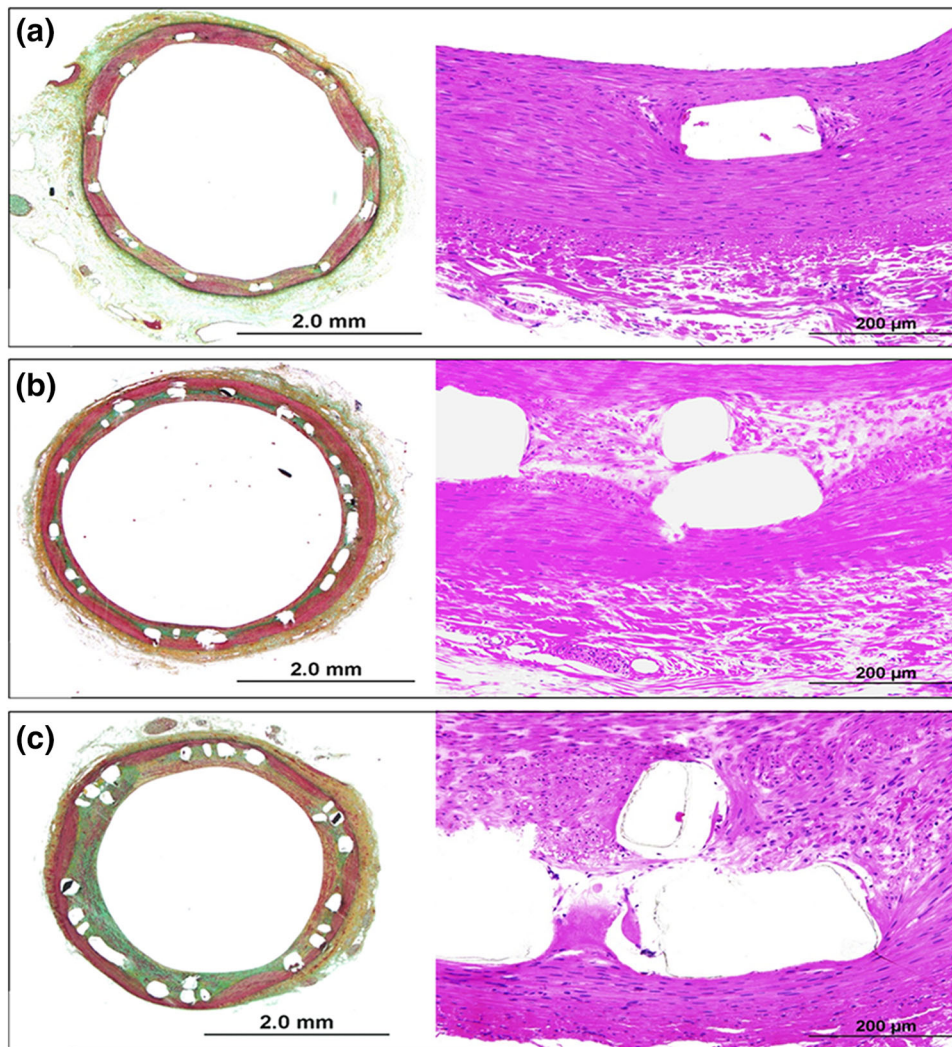


FIGURE 5. Representative histological micrographs of stented porcine arteries at 90 days. (a) O3FA DES in single and (b) overlapped configurations compared to overlapped (c) Cypher Select™ Plus SES.

such as Sirolimus and its analogs. This coating has the advantages of being derived from natural sources, being formed without the use of chemical cross-linking agents or metal catalysts that may elicit inflammation, and which naturally hydrolyzes into fatty acid and glycerol end-products which are already plentiful and well tolerated in the surrounding tissue. A drug free variety of this coating is currently used clinically in Atrium's C-QUR surgical mesh product.⁵

The O3FA drug carrier coating contributed to device safety and efficacy compared to durable coated SES, including a reduction in the rates of granulomas at 90d. As stent design¹⁶ and strut thickness/surface area^{10,21} also impact stent performance, the superiority of O3FA DES over Cypher SES is at least partially attributed to differences in the underlying metal stent. That said, though overlap locally doubles tissue

exposure to coating material and drug, overlapped exaggerated dose O3FA DES were characterized by the same low levels of stenosis (Fig. 6a), inflammation (Fig. 6b) and injury (Fig. 6c) as in the single stent configuration and nominal dose at 90d. Thus, it seems justified to predominantly attribute the superiority of O3FA DES over the durable coated SES to fast and near complete clearance of coating and tissue associated drug within the experimental time frame.

The validity of this new paradigm is not limited to the preclinical animal model. A first-in-man clinical testing in a non-randomized, prospective, multi-center single arm trial established the safety and efficacy of the Cinatra™ O3FA Drug Eluting Coronary Stent System for the treatment of single de novo lesions in native coronary vessels (Vantage 1¹⁴). The results of these studies showed an in-stent late lumen loss of

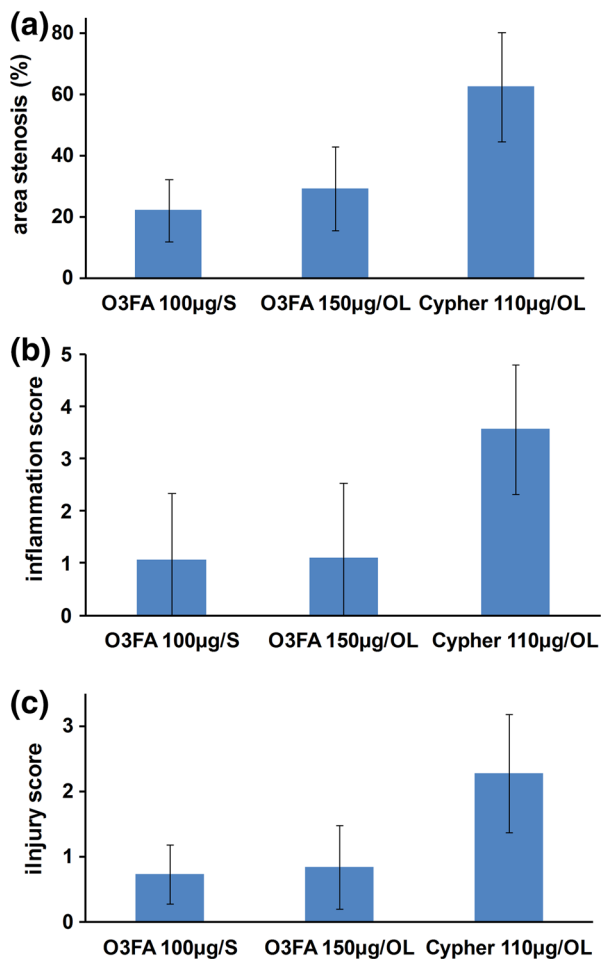


FIGURE 6. Safety in the porcine coronary model with minimal overstretch. Area of stenosis (a), inflammation score (b) and injury score (c) were evaluated at the end of 90 days for nominal dose (100 µg/stent) or exaggerated dose (150 µg/stent) O3FA DES and nominal dose (110 µg/stent) Cypher SES. Stents were deployed in single (S) or overlapped (OL) configurations. All 3 safety metrics were statistically lower for S and OL O3FA DES compared to OL Cypher/OL, $p < 0.05$.

0.25 ± 0.20 mm at 6 months and 0.26 ± 0.24 mm at 18 months in the same patients. By comparison, reported in-stent lumen loss for Cypher stents was 0.16 ± 0.37 mm at 6–8 months and 0.37 ± 0.60 mm at 2 years in the same patients.⁴ Taken together, these clinical data suggest that late lumen loss stabilizes already after 6 months in the presence of O3FA(Cinatra™ DES) and continues to rise with the Cypher stent, supporting the clinical validity of the O3FA DES product design approach.

Comparison to Second Generation Fast Eluting Durable Coated SES

While we used Cypher as a comparator durable coated SES, it is informative to contrast our findings on the O3FA DES with published findings on the

Endeavor Stent, the only FDA approved fast eluting durable coated stent. Both O3FA DES and Endeavor elute Sirolimus analogs and have thinner struts relative to Cypher (85 and 91 vs. 140 µm). Though the porcine release kinetics of Endeavor¹⁵ are slower than those of the O3FA DES (Fig S6A) the latter achieve a tissue retention profile that is intermediate between Endeavor and its slow eluting variant Resolute¹⁵ (Fig S6B).

Given that Resolute sustains Zotarolimus for longer periods in the tissue than its fast eluting counterpart, it is not surprising that it inhibits neointimal thickness at 6 months more effectively than Endeavor.⁸ While this does suggest that slow drug elution confers an efficacy advantage for durable coated SES, this paradigm does not necessarily extend to erodible coated stents as these gradually revert to a bare metal state. Indeed, during the first 28d of implantation Resolute and O3FA DES provide comparable drug tissue levels (Fig S6B), even as 85% of the O3FA coating absorbed. Thus, it may well be that fast elution is advantageous for SES with fast erodible coatings.

Moreover, Byrne *et al.*⁴ found that, durable coated PES, SES and Resolute exhibited higher late lumen loss at 2 years compared to 6 months, whereas late lumen loss stabilized after 6 months for polymer free Zotarolimus eluting stent (similar to the first in man experience with O3FA DES). Thus, even the advantages of slow elution from durable coatings may be transient.

Comparison to a Fourth Generation Erodible Coated SES

Contrasting of O3FA DES to SYNERGY stents further highlights the uniqueness of the former in the landscape of erodible coated DES. Both SYNERGY and O3FA DES have thin struts (74 vs. 85 µm), and employ an erodible coating to elute similar loads of distinct Sirolimus analogs (5.7 µg/mm Everolimus²⁸ vs. 5.8 µg/mm Corolimus). Moreover, both release their drug loads prior to full coating absorption, rendering their comparison even more relevant. SYNERGY releases 50 and >95% of its drug load by 28 and 90d,²⁸ slower than durable coated Cypher SES, while O3FA DES achieves these targets by 5 h and 8d. Moreover, whereas the O3FA DES coating begins to rapidly absorb upon implantation with only 15% remaining at 8d, the PLGA coating is relatively biostable up to 28d and achieves 85% erosion only after 90d.²⁸

Thus, both DES deliver their drug load concomitant with 85% coating erosion, but SYNERGY does so at an approximately 11-fold longer duration (90 vs. 8d). Correspondingly, SYNERGY stents provide a near constant Everolimus concentration in subjacent tissue, 1–2 µg/g, between 5 and 90d,²⁸ whereas tissue levels of

Corolimus were only detectable up to 56d post O3FA DES implantation. Correspondingly, the published 90d data for the O3FA are non-inferior and perhaps better than SYNERGY under overlap in pig coronary arteries²⁸ (0.21 ± 0.14 mm vs. 0.46 ± 0.22 neointimal thickness and 29.29 ± 13.72 vs. $46.15 \pm 18.03\%$ stenosis). Thus, a comparison of O3FA DES to SYNERGY is supportive of our hypothesis that biocompatibility of O3FA compared favorably to synthetic polymers such as PLGA and (B) that there is an advantage to delivering Sirolimus analog Corolimus at a fast rate compared to Cypher.

Study Limitations

Benchtop, computational and even animal models add insight into the factors affecting stent based drug delivery and tissue responses, but are nevertheless simplifications of the clinical scenario. In particular, we implanted DES in healthy animal vessels and used a computational model of drug distribution that idealizes the arterial wall as being compositionally uniform. Though atherosclerosis can impact drug retention and distribution, such effects seem to be more common for Paclitaxel than for Sirolimus.²³ Also, evaluation of coating erosion in rabbit iliac arteries, limits the ability to correlate with erosion with drug release and distribution in coronary pig arteries, and the choice of time points provides limited insights into erosion between 5 h and 8d. Finally, though the first in man results are promising, a clinical trial involving many more patients would be required to truly compare the O3FA platform against Cypher and other SES.

CONCLUSIONS

This study illustrates the importance of coating material choice in determining the clinical effects of DES. Safety is dominated by coating material biocompatibility and degradability and to a lesser extent by drug release kinetics. Interestingly, computational modeling of the *in vivo* data inferred that Corolimus and Sirolimus are governed by virtually identical diffusion and binding forces and are retained in the tissue through binding to specific receptors. Drug binding to high affinity receptors provides a mechanism of prolonged retention almost irrespective of stent coating properties, and potentially after bolus delivery from catheters and coated balloons.³ These findings pave the way to the incorporation of new stent coating material types and designs. Fatty acids represent a promising material family owing to their biocompatibility, degradability and ease of manipulation and formulation protocols.

ELECTRONIC SUPPLEMENTARY MATERIAL

The online version of this article (doi:[10.1007/s10439-015-1435-z](https://doi.org/10.1007/s10439-015-1435-z)) contains supplementary material, which is available to authorized users.

ACKNOWLEDGMENTS

This study was supported in part by grants from the NIH (R01 GM-49039) to ERE and in part by support of animal work and preclinical studies at MIT, CBSET and CVPath. ERE and RV are paid consultants to Atrium. Coauthors KMF, GM, TA, PM, S. Conroy and S. Corbeil are employees of Atrium Medical Corporation and provided input into the study design and editorial input into the writing of the manuscript. Data collection, analysis and interpretation of animal and computer experiments were all performed independent of input from Atrium Medical Corporation. The decision to submit the paper for publication came from joint discussions between Atrium Medical management and all authors. The authors would like to acknowledge Alicia Dale, Roger Labrecque and Jessica Mayer from Atrium Medical Corporation for assistance in executing experimental work to support this publication.

REFERENCES

- ¹Agrawal, C. M., and K. A. Athanasiou. Technique to control pH in vicinity of biodegrading PLA-PGA implants. *J. Biomed. Mater. Res.* 38:105–114, 1997.
- ²Axel, D. I., W. Kunert, C. Goggelmann, M. Oberhoff, C. Herdeg, A. Kuttner, D. H. Wild, B. R. Brehm, R. Riessen, G. Koveker, and K. R. Karsch. Paclitaxel inhibits arterial smooth muscle cell proliferation and migration in vitro and in vivo using local drug delivery. *Circulation* 96:636–645, 1997.
- ³Buerke, M., M. Guckenbiehl, H. Schwertz, U. Buerke, M. Hilker, H. Platsch, J. Richert, S. Bomm, G. A. Zimmermann, S. Lindemann, U. Mueller-Werdan, K. Werdan, H. Darius, and A. S. Weyrich. Intramural delivery of Sirolimus prevents vascular remodeling following balloon injury. *Biochim. Biophys. Acta* 1774:5–15, 2007.
- ⁴Byrne, R. A., R. Iijima, J. Mehili, S. Piniack, O. Bruskina, A. Schomig, and A. Kastrati. Durability of antirestenotic efficacy in drug-eluting stents with and without permanent polymer. *JACC Cardiovasc. Interv.* 2:291–299, 2009.
- ⁵Deeken, C. R., K. M. Faucher, and B. D. Matthews. A review of the composition, characteristics, and effectiveness of barrier mesh prostheses utilized for laparoscopic ventral hernia repair. *Surg. Endosc.* 26:566–575, 2012.
- ⁶Drachman, D. E., E. R. Edelman, P. Seifert, A. R. Groothuis, D. A. Bornstein, K. R. Kamath, M. Palasis, D.

- Yang, S. H. Nott, and C. Rogers. Neointimal thickening after stent delivery of paclitaxel: change in composition and arrest of growth over six months. *J. Am. Coll. Cardiol.* 36:2325–2332, 2000.
- ⁷Finn, A. V., F. D. Kolodgie, J. Harnek, L. J. Guerrero, E. Acampado, K. Tefera, K. Skorija, D. K. Weber, H. K. Gold, and R. Virmani. Differential response of delayed healing and persistent inflammation at sites of overlapping sirolimus- or paclitaxel-eluting stents. *Circulation* 112:270–278, 2005.
- ⁸Guagliumi, G., H. Ikejima, V. Sirbu, H. Bezerra, G. Musumeci, N. Lortkipanidze, L. Fiocca, S. Tahara, A. Vasileva, A. Matiashvili, O. Valsecchi, and M. Costa. Impact of drug release kinetics on vascular response to different zotarolimus-eluting stents implanted in patients with long coronary stenoses: the LongOCT study (Optical Coherence Tomography in Long Lesions). *JACC Cardiovasc. Interv.* 4:778–785, 2011.
- ⁹Joner, M., A. V. Finn, A. Farb, E. K. Mont, F. D. Kolodgie, E. Ladich, R. Kutys, K. Skorija, H. K. Gold, and R. Virmani. Pathology of drug-eluting stents in humans: delayed healing and late thrombotic risk. *J. Am. Coll. Cardiol.* 48:193–202, 2006.
- ¹⁰Kolandaivelu, K., R. Swaminathan, W. J. Gibson, V. B. Kolachalama, K. L. Nguyen-Ehrenreich, V. L. Giddings, L. Coleman, G. K. Wong, and E. R. Edelman. Stent thrombogenicity early in high-risk interventional settings is driven by stent design and deployment and protected by polymer-drug coatings. *Circulation* 123:1400–1409, 2011.
- ¹¹Neamtu, I., A. P. Chiriac, A. Diaconu, L. E. Nita, V. Balan, and M. T. Nistor. Current concepts on cardiovascular stent devices. *Mini Rev. Med. Chem.* 14:505–536, 2014.
- ¹²NRC (National Research Council). Guide for the Care and Use of Laboratory Animals, 1996.
- ¹³Oberhauser, J. P., S. Hossainy, and R. J. Rapoza. Design principles and performance of bioresorbable polymeric vascular scaffolds. *EuroIntervention* 5(Suppl F):F15–F22, 2009.
- ¹⁴Ormiston, J., M. Webster, F. De Vroey, S. El Jack, J. Stewart, and P. Ruygrok. Vantage 1 trial: a FIM evaluation of the cinatra corolimus-eluting stent with a bioabsorbable omega-3 fatty acid coating in de novo coronary lesions. *Heart Lung Circ.* 20:414, 2011.
- ¹⁵Parker, T., V. Dave, and R. Falotico. Polymers for drug eluting stents. *Curr. Pharm. Des.* 16:3978–3988, 2010.
- ¹⁶Rogers, C., and E. R. Edelman. Endovascular stent design dictates experimental restenosis and thrombosis. *Circulation* 91:2995–3001, 1995.
- ¹⁷Rorabacher, D. B. Statistical treatment for rejection of deviant values: critical values of Dixon's "Q" parameter and related subrange ratios at the 95% confidence level. *Anal. Chem.* 63:139–146, 1991.
- ¹⁸Schwartz, R. S., E. R. Edelman, A. Carter, N. Chronos, C. Rogers, K. A. Robinson, R. Waksman, J. Weinberger, R. L. Wilensky, D. N. Jensen, B. D. Zuckerman, and R. Virmani. Drug-eluting stents in preclinical studies: recommended evaluation from a consensus group. *Circulation* 106:1867–1873, 2002.
- ¹⁹Shazly, T., V. B. Kolachalama, J. Ferdous, J. P. Oberhauser, S. Hossainy, and E. R. Edelman. Assessment of material by-product fate from bioresorbable vascular scaffolds. *Ann. Biomed. Eng.* 40:955–965, 2012.
- ²⁰Strom, T., T. Shokati, J. Klawitter, K. Hoffman, H. M. Schiebel, and U. Christians. Structural identification of SAR-943 metabolites generated by human liver microsomes in vitro using mass spectrometry in combination with analysis of fragmentation patterns. *J. Mass Spectrom.* 46:615–624, 2011.
- ²¹Tanigawa, J., P. Barlis, K. Dimopoulos, M. Dalby, P. Moore, and C. Di Mario. The influence of strut thickness and cell design on immediate apposition of drug-eluting stents assessed by optical coherence tomography. *Int. J. Cardiol.* 134:180–188, 2009.
- ²²Tzafirri, A. R., A. D. Levin, and E. R. Edelman. Diffusion-limited binding explains binary dose response for local arterial and tumour drug delivery. *Cell Prolif.* 42:348–363, 2009.
- ²³Tzafirri, A. R., N. Vukmirovic, V. B. Kolachalama, I. Astafieva, and E. R. Edelman. Lesion complexity determines arterial drug distribution after local drug delivery. *J. Control Release* 142:332–338, 2010.
- ²⁴Tzafirri, A. R., A. Groothuis, G. S. Price, and E. R. Edelman. Stent elution rate determines drug deposition and receptor-mediated effects. *J. Control Release* 161:918–926, 2012.
- ²⁵Virmani, R., F. Liistro, G. Stankovic, C. Di Mario, M. Montorfano, A. Farb, F. D. Kolodgie, and A. Colombo. Mechanism of late in-stent restenosis after implantation of a paclitaxel derivate-eluting polymer stent system in humans. *Circulation* 106:2649–2651, 2002.
- ²⁶Virmani, R., G. Guagliumi, A. Farb, G. Musumeci, N. Grieco, T. Motta, L. Mihalcsik, M. Tespili, O. Valsecchi, and F. D. Kolodgie. Localized hypersensitivity and late coronary thrombosis secondary to a sirolimus-eluting stent: should we be cautious? *Circulation* 109:701–705, 2004.
- ²⁷Wilson, G. J., G. Nakazawa, R. S. Schwartz, B. Hui-bregtse, B. Poff, T. J. Herbst, D. S. Baim, and R. Virmani. Comparison of inflammatory response after implantation of sirolimus- and paclitaxel-eluting stents in porcine coronary arteries. *Circulation* 120(141–9):1–2, 2009.
- ²⁸Wilson, G. J., A. Marks, K. J. Berg, M. Eppihimer, N. Sushkova, S. P. Hawley, K. A. Robertson, D. Knapp, D. E. Pennington, Y. L. Chen, A. Foss, B. Hui-bregtse, and K. D. Dawkins. The SYNERGY biodegradable polymer everolimus eluting coronary stent: porcine vascular compatibility and polymer safety study. *Catheter. Cardiovasc. Interv.* 2015. doi:10.1002/ccd.25993.